ADVANCED FUNCTIONAL MATERIALS
www.afm-journal.de

Materials Views
www.MaterialsViews.com

Structural and Biomimetic Chemical Kinetics: Kinetic Magnitudes Include Structural Information

Toribio F. Otero and Jose G. Martinez*

Electrochemical reactions in films of conducting polymers involve reactive chains, exchanging ions and solvent with the electrolyte under current flow. The reaction induces structural changes: conformational movements in chains and swelling, shrinking, compaction, and relaxation processes in the reactive dense gel. Conformational movements and structural changes induced by reactions are not included by today's chemical kinetic models. Using different packed conformations as initial states for the study of the reaction kinetics in films of different conducting polymers, rate coefficients, activation energies, and reaction orders related to the concentration of active centers in the film change with the structure of the selected initial state. The kinetic magnitudes include and quantify conformational and structural energetic states. Therefore, the reaction activation energy includes the constant reaction activation energy and the conformational energy of the initial packed state. The electrochemically stimulated conformational relaxation model describes the empirical variation of the kinetic magnitudes.

1. Introduction

New, reactive (electrochemical) and biomimetic devices such as batteries,[1,2] smart windows,[3,4] smart membranes,[5,6] artificial muscles,[7,8] nervous interfaces,[9,10] or drug delivery systems[11] are being produced from conducting polymers (CP) and electrolytes (liquid, gel, or solid). Two main facts are present during the electrochemical actuation of any of those devices: a) the chemical composition (polymer-ion-solvent) of the CP films shifts and b) interactions between electric currents and chemical reactions in the film involve reactive polymer chains, conformational movements of the chains, ionic exchange, and solvent exchange between the film and the electrolyte. A similar variation exists and analogous events occur during reactions in living cells from biological organs. Most of the biological reactions involving reactive biopolymers induce conformational movement of the reactive chains. The main difference is that in biology the action is triggered by ions delivered from nerves (providing differential electrical and chemical information) instead of the electronic exchange with metals from films of conducting polymers[12] triggering the electrochemical reaction.

In this context actuation related to reactive conducting polymers means generation of movements in artificial muscles; charge/discharge in batteries; absorbance, transmittance, or reflectance change in smart windows; porosity or permselectivity variation in smart membranes; transducting and translating electronic pulses into specific ionic pulses, and vice-versa, all taking place under faradic control of each device actuation.[13–19]

Quantitative descriptions of those biomimetic devices, or of the parallel biological reactions and functions, are outside current chemical and physico-chemical models. In our laboratory we are exploring chemical kinetic methodologies applied to conducting polymers, including structural aspects such as swelling, shrinking, compaction, or relaxation induced by the electrochemical reaction in order to develop structural chemical and electrochemical kinetics.[20–31] As reactive dense gels, any conducting polymer can be considered as a material model (only one reactive macromolecule, one anion, one cation, and one solvent) for the study of biomimetic chemical kinetics.

1.1. Driving Reactions

Actuation in any of those biomimetic devices which constitutive conducting polymers experience a prevalent exchange of balancing anions with the electrolyte during p-doping is driven by the following oxidation/reduction reactions:[13,16,28]

$$(\mathrm{Pol}^{*}) + n(\mathrm{A}^{-}) + m(\mathrm{S}) \rightleftarrows \left[(\mathrm{Pol}^{n+})(\mathrm{A}^{-})_n(\mathrm{S})_m\right]_{\mathrm{gel}} + n\mathrm{e}^{-}_{\mathrm{metal}} \quad (1)$$

where Pol^{*} represents the active centers in the polymeric chains of the film, understood as those places along the polymeric chains that are able to store a positive charge after oxidation; A^{-} is the anion exchanged with the electrolyte for charge balance inside the film (n anions are exchanged to compensate the n electrons removed from the polymeric chains that generate n positive charges); S represents a solvent molecule (m molecules of solvent are exchanged for osmotic balance); and the subscript gel indicates that the material is an expanded gel and the subscript metal indicates that the extracted electrons are transported by a metallic substrate.

Prof. T. F. Otero, J. G. Martinez
Center for Electrochemistry
and Intelligent Materials (CEMI)
Universidad Politécnica de Cartagena (UPCT)
Aulario II, E-30203, Spain
E-mail: toribio.fotero@upct.es

DOI: 10.1002/adfm.201200719

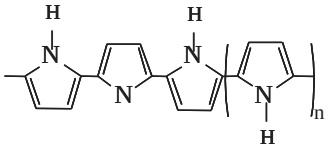

Scheme 1. Ideal neutral polypyrrole chain. Reproduced with permission.[13] Copyright 1999, Kluwer Academic/Plenum.

Similar reactions can be written for conducting polymer-macroanion blends exchanging cations during p-doping[15–17,22] or for CPs exchanging cations during n-doping[20,21,32–42]. Conclusions here attained from reaction 1, can be translated also to those polymers exchanging cations during reactions.

1.2. Reaction-Induced Structural Changes

Scheme 1 represents the structure of an ideal lineal chain of neutral polypyrrole where rotations between two consecutive monomeric units, C–C σ bonded, are allow.

The oxidation of this benzenoid structure promote the change of the double bond distribution getting flat electron delocalized quinoid structures (polarons) represented by **Scheme 2**.

Rotations between consecutive monomeric units become hindered inside the new structure: conformational structural changes (**Figure 1**) are induced by the electrochemical oxidation. Reaction (1) can be expressed as **Scheme 3**.

Reaction-induced conformational movements allow structural bidimensional (Figure 1) representations of the reaction.

When the chains take part of films the oxidation induces (Figure 1b) 3D structural relaxation of the chains and swelling of the film: free volume must be generated to lodge the counterions arriving from the solution and that are required for charge balance. During the electrochemical reduction, electrons are injected to the polymer chains, the positive charges are eliminated, the counterions are expelled towards the solution, and the film shrinks from the strong polymer-polymer attractive forces. The average distance between chains becomes shorter than the counterion diameter when the film still is partially oxidized and the structure closes. Being a soft material with a high percentage of reduced structures (structure 1 allowing free rotation between consecutive monomeric units) a slow reduction and subsequent conformational compaction of the polymeric structure goes on at high cathodic overpotentials. Therefore, conformational movements in chains and macroscopic swelling, shrinking, closing, and compactation of the films are structural changes induced by reactions.[13,44,45] Reversible macroscopic dimensional changes induced in films of conducting polymers by electrochemical reactions are being followed using different experimental methodologies.[46–60]

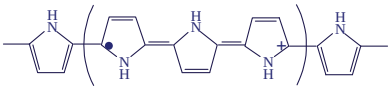

Scheme 2. Polaron generated in a polypyrrole chain. Reproduced with permission.[13] Copyright 1999, Kluwer Academic/Plenum.

Toribio F. Otero received his PhD in Chemistry in 1978 from the Complutense University of Madrid. His thesis was supervised at the Institute Rocasolano from the CSIC. In 1989 he became a Full Professor of Physical Chemistry and Macromolecules at the University of the Basque Country. In 2002 he became a Full Professor of Physical Chemistry at the Technical University of Cartagena. His work mainly concerns electrogeneration, electrochemical properties, electrochemical applications, and theoretical modelling of conducting polymers.

Jose G. Martinez received a degree in electronic technical engineering in 2007 and a degree in automatics and electronics engineering in 2009 both from Technical University of Cartagena. Currently he is pursuing his PhD in biomimetic devices from conducting polymers.

1.3. Reactants

In Reaction (1) the reactants are the active centers (Pol∗) along the chains (most of them inside the film) and the anions (A^-) in solution. The electron transfer only occurs, under anodic or cathodic overvoltages, when both reactants can meet simultaneously inside the film. Thus, if the anion present in the electrolyte is too big, the conformational movements cannot generate enough free volume to allow its penetration into the film and the oxidation does not take place, even at high anodic overpotentials.[45]

1.4. Shift of the Intermolecular Interaction

A first consequence of the simultaneous emerging positive charges and conformational movements in chains during reaction is the continuous shift of the magnitudes of the crossed intermolecular interactions between chains, solvent, and ions inside the reactive gel. A second consequence is that the reaction kinetics (activation energy, reaction orders, and reaction constants) can include quantitative information about both structural changes (conformational compaction, relaxation, shrinking, and swelling) and intermolecular interaction variations along the reaction.

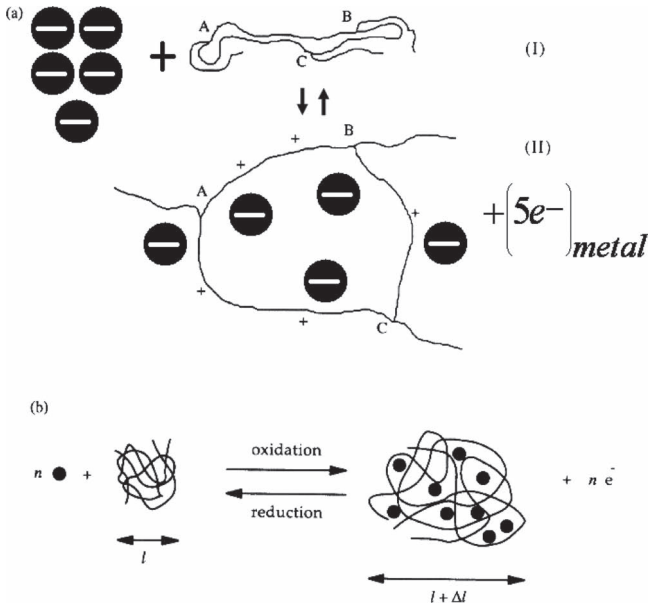

Figure 1. Electrochemically stimulated conformational changes. a) A crosslinked structure stores five positive charges during oxidation generating, by conformational movements, the free volume required to store five anions penetrating from the solution and five electrons are transfer to the metal. b) Similar structural changes from a 3D structure. Reverse processes occur during electrochemical reduction. Reproduced with permission.[43]

In this context, the solvent cannot be considered as a reactant in the restrictive sense that its chemical structure suffers deep changes during Reaction (1). Nevertheless, it can have, as in most biological reactions do, a great influence on the reaction kinetics. Getting more packed or swollen structures for reduced or oxidized states, in different solvents, should depend of the polymer-solvent and ion-solvent interactions inside the films. When those different structures are used as initial states for oxidation or reduction reactions, respectively, different reaction rates should be expected keeping a constant value for the rest of the variables acting on the reaction rate.

Here, chemical kinetic methodologies will be revisited and described when the chemically induced structural changes are considered. The empirical variation of the reaction activation energy, the reaction coefficient (reaction constant), or the reaction orders as a function of the packed conformational structure of the initial state for the reaction will be studied and quantitatively justified.

2. Reaction Kinetics

The empirical oxidation reaction rate of a conducting polymer film (here polypyrrole) according with Reaction (1) is:

$$r = \frac{\mathrm{d}\left[\mathrm{Pol}^{+}\right]}{\mathrm{d}t} = -\frac{\mathrm{d}\left[\mathrm{Pol}^{*}\right]}{\mathrm{d}t} = k\left[\mathrm{A}^{-}\right]^{\alpha}\left[\mathrm{pPy}^{*}\right]^{\beta} \tag{2}$$

where k (L mol^{-1} s^{-1}) is the rate coefficient of the oxidation reaction; r (mol s^{-1} L^{-1}) is the oxidation reaction rate; α is the reaction order related to the counterion concentration in solution; β is the reaction order related to the polymer active centers; and [Pol*] is the concentration of active centers in the polymer film.

The charge consumed to oxidize the film, Q_{ox} (C), allows the obtention of this concentration variation along the reaction time:[27]

$$\left[\mathrm{Pol}^{*}\right] = \frac{Q_{ox}\rho}{mF} \tag{3}$$

where m is the mass of the polymer film, ρ is the density of the reduced polymer usually obtained by flotation,[61] and F is the Faraday constant (96 485, C mol^{-1}). Considering that the consumed charge depends of the anodic current flowing through the polymer, i (A), at any time, Equation (2) becomes:

$$r = -\frac{\mathrm{d}\left[\mathrm{Pol}^{*}\right]}{\mathrm{d}t} = \frac{\rho}{mF}\frac{\mathrm{d}Q_{ox}}{\mathrm{d}t} = \frac{i\rho}{mF} \tag{4}$$

The film volume and density change along Reaction (1). Even if the average change of volume in the CPs during the reaction is as low as 1%, for the design of electrochemical devices such as artificial muscles, batteries, and supercapacitors it results in the more convenient use of specific magnitudes: per unit of mass

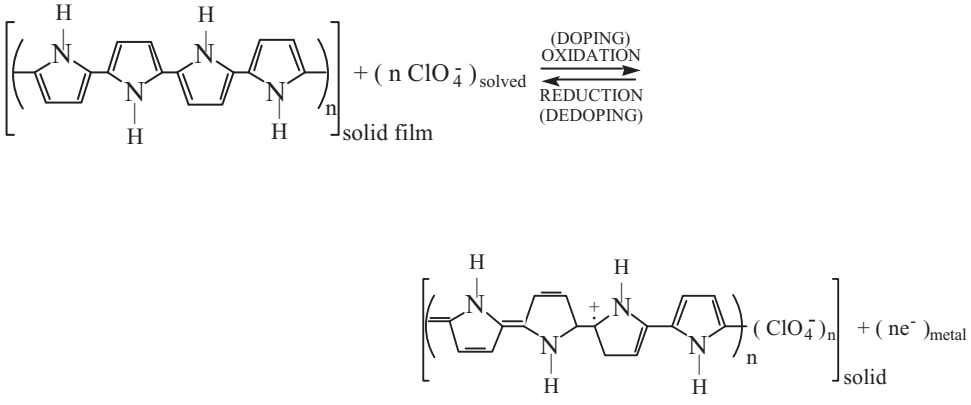

Scheme 3. Reaction (1).

of the reduced and dried material. The specific concentration of active centers (mol g^{-1}) is:

$$[\mathrm{Pol}^*] = \frac{Q_{ox}}{mF} \quad (5)$$

Being m the mass of the reduced and dry polymer material. The specific reaction rate (mol s^{-1} g^{-1}) becomes:

$$r = \frac{i}{mF} \quad (6)$$

Equations (4) and (6) show the instantaneous oxidation and reduction rates at any intermediate reaction time between two well-defined (initial reduced and final oxidized) states of the film, which are determined by the current flowing through the film after that time.

By taking logarithms in Equation (2):

$$\log(r) = \log(k) + \alpha \log[\mathrm{A}^-] + \beta \log[\mathrm{Pol}^*] \quad (7)$$

Equation (7) indicates the experimental procedure that can be followed to check whether Reaction (1) occurs under chemical kinetic control and to obtain the kinetic magnitudes; α can be obtained by changing the electrolyte concentration [A^-] under constant temperature (log k = constant) and constant concentration of active centers in the film (β log[Pol*] = constant). The consumption of a constant concentration of active centers requires (Equations (4) and (5)) the flow of the same charge to go from the same initial state to the same final state everytime.

Under those conditions, Equation (7) becomes:

$$\log(r) = \log(k') + \alpha \log[\mathrm{A}^-] \quad (8)$$

Where log (k') = log (k) + βlog [Pol*] and

$$k = \frac{k'}{[\mathrm{Pol}^*]^\beta} \quad (9)$$

Equation (8) states that when the reaction occurs under chemical kinetic control a double logarithmic variation is expected between the experimental reaction rates and the studied electrolyte concentrations. The slope is the reaction order α and the intercept at [A^-] = 0 defines the constant k', which allows calculation of the reaction coefficient k using Equation (9).

Working under constant temperature and constant concentration of counterions in solution (αlog[A^-] = constant) and changing the concentration of active centers, [Pol*], by consumption, Equation (5), of different oxidation charges, Equation (7) becomes:

$$\log(r) = \log(k'') + \beta \log[\mathrm{Pol}^*] \quad (10)$$

where log (k'') = log (k) + αlog [A^-] and

$$k = \frac{k''}{[\mathrm{A}^-]^\alpha} \quad (11)$$

By using the values of α and intercepts from the log(r) vs log[Pol*] plot, the rate coefficient k can be obtained from Equation (11).

Finally, by including the Arrhenius reaction constant, $k = A\exp\left(-E_a/RT\right)$, Equation (7) becomes

$$\ln r = \ln \mathrm{A} - \frac{E_a}{RT} + \alpha \ln[\mathrm{A}^-] + \beta \ln[\mathrm{pPy}^*] \quad (12)$$

Where A is the pre-exponential factor, E_a is the activation energy, R is the universal gas constant (R = 8.314 J K^{-1} mol^{-1}), and T is the temperature.

Indicating that changing the temperature, keeping the rest of experimental conditions constant and working under constant concentrations of electrolyte and active centers,

$$\log r = \log k''' - \frac{E_a}{RT} \quad (13)$$

with log k''' = log A + αlog [A^-] + βlog [Pol*] and $k = \frac{k'''}{[\mathrm{A}^-]^\alpha[\mathrm{Pol}^*]^\beta}$

Equation (13) indicates that a semilogarithmic dependence is expected between the oxidation reaction rate and (T^{-1}) when working under a constant concentration of reactants. The activation energy is then obtained from the slope and the reaction coefficient, k, from the intercept, and the reactant concentrations.

2.1. Reactive Gels: Initial Structural State for the Oxidation

The above-described chemical kinetic methodology can be found in chemical, biological, or electrochemical books. Now the existence of swollen/shrunk and conformational packed structures (**Figure 2**) in reactive films of CPs provides new kinetic possibilities.[20–31] Different reduced equilibrium states

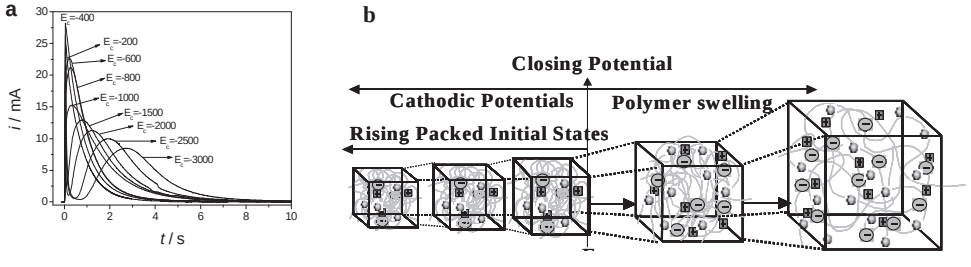

Figure 2. a) Chronoamperometric responses from a PEDOT coated platinum electrode in 0.1 M $LiClO_4$ acetonitrile solution, submitted to potential steps from different cathodic potentials and held for 30 s each time, to 500 mV. Reproduced with permission.[31] Copyright 2010, Society of Chemical Industry. b) Volume variations of a cubic volume inside the PEDOT film after polarization, for a constant time, at rising cathodic overpotentials. Initial states with rising packed conformations (left side of the closing potential) give slower oxidation reactions, by potentials step to the same oxidation potential, showing two chronoamperometric maxima. Adapted with permission.[31] Copyright 2010, Society of Chemical Industry..

with an open structure, attained by reduction at potentials on the right side of the closing potential for the same reduction time, can be used as initial states. The kinetic procedure deduced from Equation (7) for different [A^-] (Equation (8)), or different [Pol*] (Equation (10)) or different temperatures (Equation (13)) can be repeated from different initial states to attain, every time, the kinetic magnitudes: k, E_a, α, and β.

By reduction at higher cathodic potentials than the closing potential,[20–21,24,26,29–31] or for higher reduction times at the same potential,[25,61] more reduced and packed conformational structures are obtained. The packed conformations are not equilibrium states: longer polarization times produce deeper packed conformational structures. Nevertheless, the energy consumed to pack the structure stabilizes the attained state. It behaves as if it is in a frozen state: only after supplying the oxidation energy required to relax the structure free volume, required to lodge charge balance counterions, can it be generated and the oxidation becomes possible. Thus, when after reduction/packing the polarization is switched off, the attained packed state is stable inside electrolytes or in gases for several minutes.[62–64] After switching off the electric contact, the reduced and packed film can be extracted from the solution into the nitrogen atmosphere of the cell for some time, then it is put back into the solution and used as an initial state for the oxidation reaction by potential step. The anodic chronoamperommetric response (the oxidation kinetics) overlaps with that obtained just after reduction compaction inside the electrolyte. In conclusion, conformational packed states of a film attained by reduction at the same potential for the same time under constant temperature can be used as a reproducible initial state for the subsequent kinetic study, even if it is not an equilibrium state. Again the kinetic procedure for different [A^-] (Equation (8)), or different [Pol*] (Equation (10)) or different temperatures (Equation (13)) can be repeated from a different initial state of packed conformations every time to obtain the kinetic magnitudes: k, E_a, α, and β, for each of the studied packed conformations.

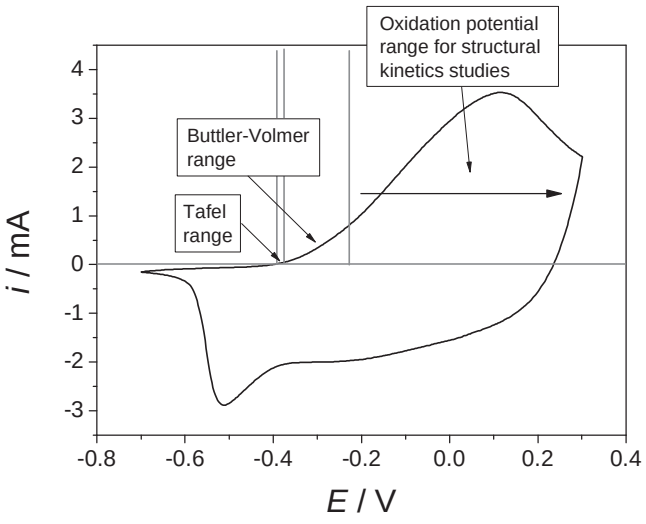

Figure 3. Stationary voltammetric response of a polypyrrole film. Potential ranges where the oxidation kinetics are usually studied: Tafel region (linear dependence i/η), Butler-Volmer region (ln i/η), or different oxidation states used in this review.

2.2. Final Oxidized States: Concentration of the Active Centers in the Film

The concentration of active centers in the initial state is calculated (Equations (4) and (5)) from the charge consumed during the oxidation process. The easiest way to know the potential range where the oxidation/reduction of conducting polymers takes place and the potential range where the concentration of active centers can be shifted without film damaging (by overoxidation) in electrolytes is by cyclic voltammetry. **Figure 3** shows the stationary voltammetric response of a polypyrrole film after three consecutive cycles. Positive currents define oxidation kinetics; negative currents define reduction kinetics.

Electrochemical kinetic equations state the evolution of the current (the reaction rate) as a function of the overpotential, η.[65,66] Figure 3 shows the potential range for the Tafel linear dependence (for $\eta < 10$ mV) and for the Buttler-Volmer semilogarithmic dependence (10 mV $< \eta <$ 150 mV). In this article, the oxidation kinetics are studied by potential steps from the selected initial reduced state to high anodic overpotentials ($\eta > 150$ mV). Thus different concentrations of active centers, close to those of the full-oxidized material, can be used to check Equation (10). Those high concentrations are representative of the working conditions in most of the electrochemical devices constituted by conducting polymers.Therefore, when required for kinetic studies (Equation (10)) the concentration of active centers is controlled by potential steps, from the same cathodic potential required to get the initial state, to increasing (and high) anodic overpotentials and determined (Equation (3)) from the charge consumed during the transition from a partially reduced initial state (equilibrium or compacted) to a final more oxidized state.

2.3. The Structure of the Initial State Controls the Oxidation Rate

The oxidation kinetics of films of CPs studied by anodic potential steps is followed by the chronoamperometric responses. Under constant chemical conditions (temperature, electrolyte concentration [A^-] and concentration of active centers [Pol*]) drastic kinetic changes are observed (Figure 2, from a PEDOT film) when the oxidation was performed from different initial states with open or raising packed conformational structures. Equation (6) states that the reaction rate at any time is a linear function of the current flowing by the system. Figure 2 corroborates that longer times with flow of lower currents (slower oxidation rates) are required for oxidation completion after reduction at more cathodic potentials. The results seem to contradict electrochemical principles: deeper reduced initial states and larger potential steps produce slower reaction rates, requiring longer times for the film oxidation completion. Similar unexpected results (chronoamperometric or voltammetric) from different conducting polymers were named from the eighties anomalous results, memory effect, relaxation processes, asymmetric processes, and so on.[45,56,63,64,67–98]

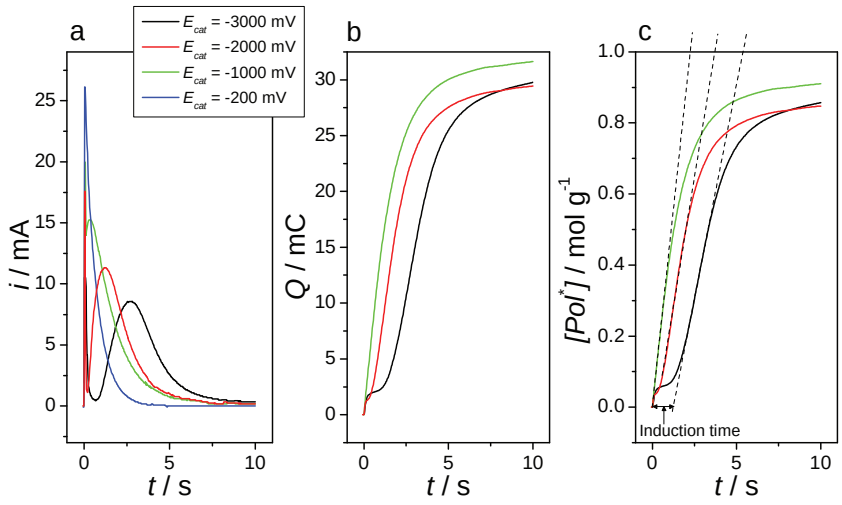

Figure 4. a) Chronoamperometric responses of a PEDOT-coated platinum electrode in 0.1 mol L^{-1} $LiClO_4$ acetonitrile solution, submitted to potential steps from different cathodic potentials kept for 30 s to 500 mV. b) Chronocoulograms obtained by integration of the experimental chronoamperograms. c) Variation of the concentration of active centers in the polymeric film with time, calculated using Equation (5). Reproduced with permission.[31] Copyright 2010, Society of Chemical Industry.

2.4. The Structure Influences the Kinetics: Initial Reaction Rate

Structural anodic chronoamperometric responses (Figure 1) show two different shapes (**Figure 4**a) when the initial state is an open (blue chronoamperogram) or compacted conformational structures (green, red, or black chronoamperograms). An initial conformational packed structures gives two maxima: the sharp initial peak is related to the charge of the electrical double layer and the second with the polymer oxidation through conformational relaxation-nucleation and coalescence processes.[13,44,98–109]

By integration of the chronoamperograms, the concomitant chronocoulograms (Q_{ox} vs. t) in Figure 4b were obtained. Through Equations (4) and (5) this figure takes the most usual representation of a chemical kinetics ($[Pol^*]/t$), shown in Figure 4c. Any chronoamperogram showing a nucleation/relaxation maximum (Figure 4a) corresponds to reaction kinetics depicting a remarkable induction time (Figure 4c).

The initial reaction rates, $d[Pol^+]/dt$, required to check Equations (8), (10), and (13) are obtained from the slope of the kinetics at the inflection point or the slope at time $t = 0$ in absence of induction time (Figure 3b). From Equation (5) and considering that $Q_{ox} = it$.

$$[Pol^*] = \frac{it}{mF} \tag{14}$$

According to Equation 6 the initial oxidation rate, $r = i/mF$ at time $t = 0$, also can be obtained from the current at the initial chronoamperometric peak (in the absence of structural effects, blue line Figure 4a) or from the current at the nucleation/relaxation maximum (green, red, or black chronoamperograms, Figure 4a) that correlates the induction time on the chronocoulogram.

3. Structural Chemical Kinetics

The full chemical kinetic methodology above described (at different temperatures, different salt concentration in solution and different concentrations of active centers in the film) can be repeated now from a different structural initial state every time. Different open conformational structures (Figure 2 right side of the closing potential) or different frozen structures of packed conformations of the chains (Figure 2 left side of the closing potential) are used as initial states. From every initial state reaction orders, reaction coefficient and activation energy are obtained for different conducting polymers and electrolytes.[20,21,23–27,29–31]

3.1. Methodology

Figure 5 presents the structural chemical kinetic methodology.

Equation (8) can be explored by choosing the initial sate A, attained by reduction of the oxidized polymer film at the same cathodic overpotential for the same reduction time at the same temperature every time. The polymer is then oxidized by stepping the potential to the same anodic overpotential in order to get the same final oxidation state 1 involving the same oxidation charge Q_{ox}. The

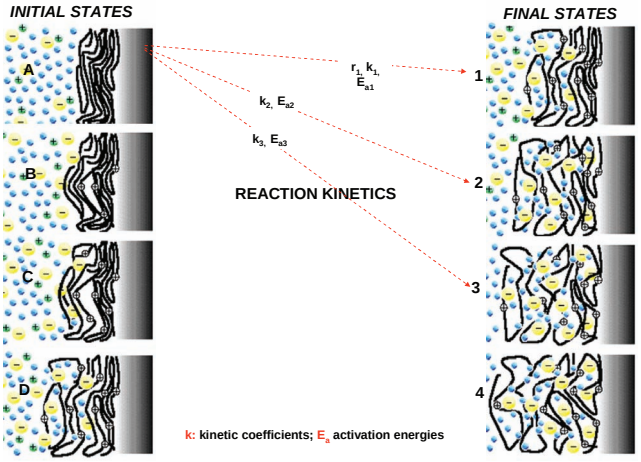

Figure 5. Different initial states of packed conformations (A, B, C, and D) and different final states of oxidation-swelling (1, 2, 3, 4) of the reactive gel. By potential step from A to 1 under different concentration of electrolyte or different temperatures (see the procedure in the text), the kinetic coefficient (k), the reaction order related to the electrolyte (α), and the activation energy (E_a) for the oxidation are obtained. By potential step from A to the different final states (1, 2, 3, 4), the reaction order related to the concentration of active centers in the film (β) is attained. By repeating the procedure from a different initial state of packed conformations every time (A, B, C and D) a new ensemble of those magnitudes is obtained. (+) denotes positive charges in chains; yellow circles show anions; green circles represent cations, and blue circles represent solvent molecules.

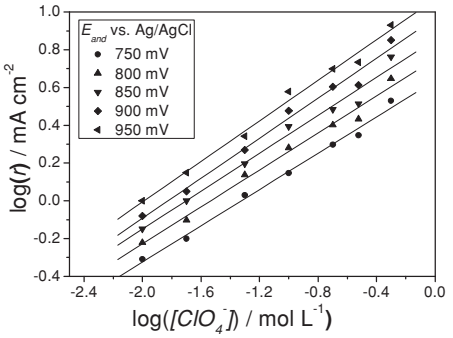

E_{and}/mV	r/mA cm^{-2}	α	k/mol l^{-1} s^{-1}	[pTh$^+$]/(mol L^{-1})
750	0.64	0.49	17.1	0.38
800	0.75	0.50	16.5	0.47
850	0.85	053	16.0	0.56
900	0.96	0.51	16.6	0.65
950	1.04	0.53	16.3	0.75

Figure 6. Double logarithmic plot of the oxidation rates of a polythiophene-coated platinum electrode versus the [$C10_4^-$]. The film was submitted to potential steps between 0.0 mV, kept for 30 s each time, and the different anodic potentials E_{and} indicated, in different concentrations of $LiClO_4$ acetonitrile solutions: 0.01, 0.025, 0.05, 0.1, 0.2, 0.3, and 0.5 M. An average slope of 0.5 (see table) is the reaction order, α, related to the electrolyte. The initial oxidation rates, r, were obtained by extrapolation to [$C10_4^-$] = 0. The kinetic constants were obtained from Equation 8 using the experimental [pTh$^+$] obtained from the total oxidation charge at every final potential using Equation 6. Similar α values were obtained from different anodic potentials. Reproduced with permission.[26] Copyright 2008, Elsevier.

oxidation kinetics are followed (Equations (8) and (12)) through the chronoamperometric response. By repeating this reduction/oxidation procedure for different concentrations of electrolyte, if the results fit Equation (8) the chemical kinetic control of the process will be corroborated and both reaction coefficient, k, and reaction order, α, can be obtained.

According with Equation (10), by stepping the potential now to increasing anodic potentials, oxidation states 1 to 4 from Figure 5 will be attained by consumption of different Q_{ox}, different concentrations of active centers (Equations (4) and (5)) from the initial state are consumed. If the attained oxidation rates fit Equation 10 the chemical kinetic control of the process will be corroborated getting the reaction order, β, from the slope and the reaction coefficient, k, from the intercept.

In order to get the activation energy (Equation (13)) the initial state for the oxidation must be attained, again, by reduction at the same potential for the same reduction time and at the same temperature every time. Then the electrode is extracted from the solution into the nitrogen atmosphere of the cell over the electrolyte.[62] The temperature of the cell is adjusted to the new experimental value and then the electrode is put back into the electrolyte and immediately submitted to the potential step (the reduction potential is only kept for 0.1 s). The procedure is repeated for the different temperatures to obtain the initial oxidation rates and the activation energy E_a.

Until here the procedure is quite similar (only a few changes to obtain the activation energy) to that descried in chemical, electrochemical, or biochemical books. The new aspect for reactive conducting polymers is that the full chemical kinetic methodology for the oxidation can now be repeated using, every time, a different structural initial state of open or compacted conformations (A, B, C, or D in Figure 5), resulting in a new series of α, β, k, and E_a values from every initial state.

4. Structural Oxidation Kinetics: Results

The described methodology has been followed using different conducting polymers and electrolytes. Results from the literature are here collected.

4.1. Influence of the Electrolyte Concentration (α and k)

The potentiostatic oxidation of polythiophene films follows (**Figure 6**) Equation (8) for different electrolyte concentrations, corroborating the chemical kinetic control of the process.[26] Every line shows the evolution of the empirical initial oxidation rate from the same initial state, attained by reduction at 0.0 mV kept for 30 s every time, to the same anodic potential (constant concentration of active centers, [pTh*]) in different concentrations of $LiCl0_4$ acetonitrile solutions: 0.01, 0.025, 0.05, 0.1, 0.2, 0.3, and 0.5 M under constant temperature. Parallel results attained for a different anodic potential every time corroborate that Equation (8) is followed whatever the final oxidation state for the oxidation. The table inserted in the figure shows that the reaction order, α, and the rate coefficient does not suffer significant changes for different final oxidation states. Similar constant values were obtained by repeating the kinetic study from different initial states of packed conformations. Analogous kinetic results were obtained for different conducting polymers: PEDOT,[31] polypyrrole in aqueous solution,[30] polypyrrole in acetonitrile,[29] poly(3-methylthiophene),[25] anthraquinone-functionalized poly(3,4-ethylenedioxythiophene),[20] and dithienylcyclopentadienone-derivative/3-methylthiopene copolymer.[31]

4.2. Influence of the Concentration of Active Centers (β and k).

The potentiostatic oxidation of poly(3-methylthiophene) films follows (**Figure 7**) Equation (10) for the consumption of different concentrations of active centers in the film, corroborating the chemical kinetic control of the process.[26] Different concentrations of active centers in the film were obtained with potential steps from the same initial state, attained by reduction at the same potential kept for 60 s every time, to a different anodic potential (600, 700, 800, 900, 1000, and 1100 mV) in 0.1 M $LiClO_4$ acetonitrile solutions every time. The different concentrations of active centers, [p3-MTh*], were obtained from Equations (10) and (17), after integration of the experimental chronoamperograms to get each oxidation charge, Q_{ox}.[25]

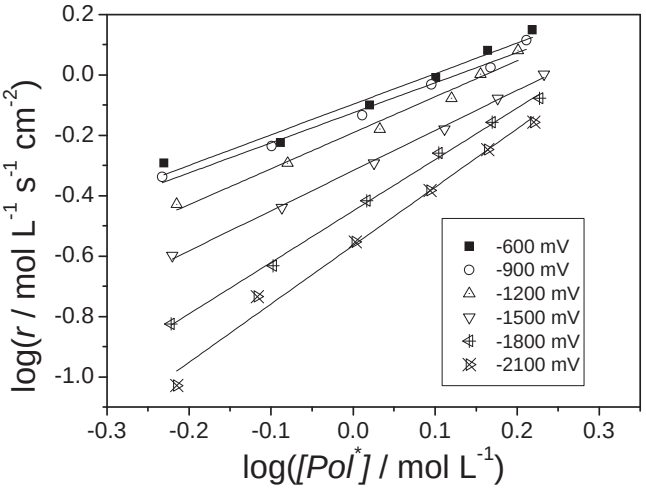

Figure 7. Oxidation of poly(3-methylthiophene) films. Double logarithmic plot of the initial oxidation rates obtained in 0.1 M $LiClO_4$ acetonitrile solutions at constant temperature by potential steps from the same initial potential, kept for 60 s, to different anodic potentials (600, 700, 800, 900, 1000, and 1100 mV) in order to consume different oxidation charges and different concentrations of active centers (Equations (10) and (17)). The procedure was repeated (different lines) from a different initial state attained by reduction at the cathodic potentials, kept by 60 s. From the slopes the activation energy for the oxidation reaction is obtained. Reproduced with permission.[25] Copyright 2007, Elsevier.

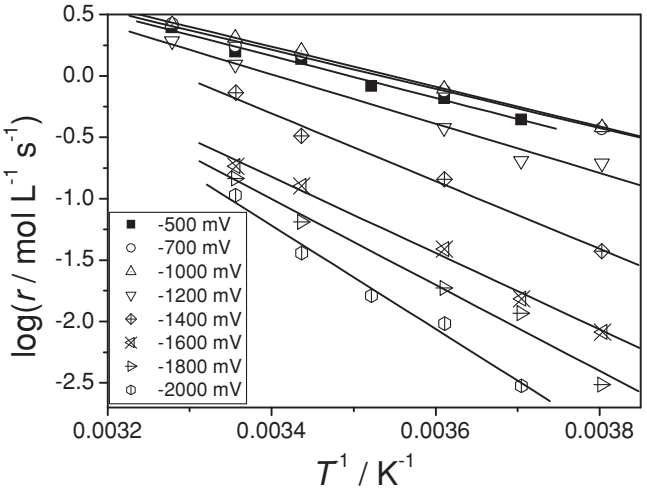

Figure 8. Arrhenius plot for the polypyrrole oxidation in 0.1 M $LiClO_4$ acetonitrile solution at –10, –3, 4, 11, 18, 25, and 32 °C. A new film was used for each temperature. Potential steps were carried out between different cathodic potentials to 200 mV, as anodic potential. From each slope (Equation (13)), a value is obtained for the activation energy. Reproduced with permission.[30] Copyright 2010,Elsevier.

The double logarithmic representation presents a different slope for each of the structural initial states. Different slopes and different origin ordinates indicate (Equation (10)) that the reaction order, which is related to the concentration of active centers (β) and the reaction kinetic coefficient (k), changes with (and can contain information about) the packed conformational structure of the initial state, opening new possibilities for chemical and biochemical kinetics. Similar empirical results were obtained from different conducting polymers: PEDOT,[31] polypyrrole in aqueous solution,[30] polypyrrole in acetonitrile,[29] poly(3-methylthiophene),[25] anthraquinone-functionalized poly(3,4-ethylenedioxythiophene),[20] and dithienylcyclopentadienone-derivative/3-methylthiopene copolymer.[31]

4.3. Temperature Influence (E_a and k)

Each line in **Figure 8** shows that the polypyrrole oxidation at different temperatures in 0.1 M $LiClO_4$ acetonitrile solutions follows Equation (13).[30] The same initial state is obtained every time by reduction at a constant cathodic potential during 60 s at 25 °C. The coated electrode is extracted from the solution into the nitrogen atmosphere of the cell while the temperature of the electrolyte is adjusted. After returning the electrode into the solution the polymer was oxidized by potential step to 200 mV.

Different slopes (activation energies) and origin ordinates (reaction coefficient, k), are attained (Equation (13)) when the kinetic study was started from a different structural initial state each time: E_a and k change with (and contain information about) the molecular structure of the initial state.

Similar empirical results were obtained from different conducting polymers: PEDOT,[31] polypyrrole in aqueous solution,[30] polypyrrole in acetonitrile,[29] poly(3-methylthiophene),[25] anthraquinone-functionalized poly(3,4-ethylenedioxythiophene),[31] and dithienylcyclopentadienone-derivative/3-methylthiopene copolymer.[21]

4.4. E_a, β, and k Contain Conformational Information

Figure 9a shows the evolution of the activation energy during the oxidation reaction, obtained from Figure 8, as a function of the potential of reduction used to obtain the initial state. Similar results were obtained from different CPs. Figure 9b shows the schematic description of results from Figure 9a. The empirical activation energy of the polymer oxidation contains two components: the constant chemical activation energy of the oxidation reaction plus the conformational activation (or conformational relaxation) energy required to relax the packed conformations generating the required free volume to lodge the counterions penetrating from the solution.

Whatever the initial state for the oxidation has an open structure (Figure 2) it gives the expected constant chemical activation energy (Figure 9b right side). When rising packed conformations were used as initial states for the oxidation, the energy required to relax the packed conformations, allowing the penetration of the balancing counterions, also increased. The potential where the conformational energy starts to grow is the closing potential. When the initial state for the oxidation was attained by reduction of the material at more positive potentials than the closing potential, the structure was open and the oxidation/swelling occured under diffusion kinetic control of the counterions inside the film. By using as initial state for the oxidation, a closed structure of packed conformations, attained by reduction at more negative potentials that the closing potential, the oxidation is initiated under conformational relaxation kinetic control, consuming the conformational activation

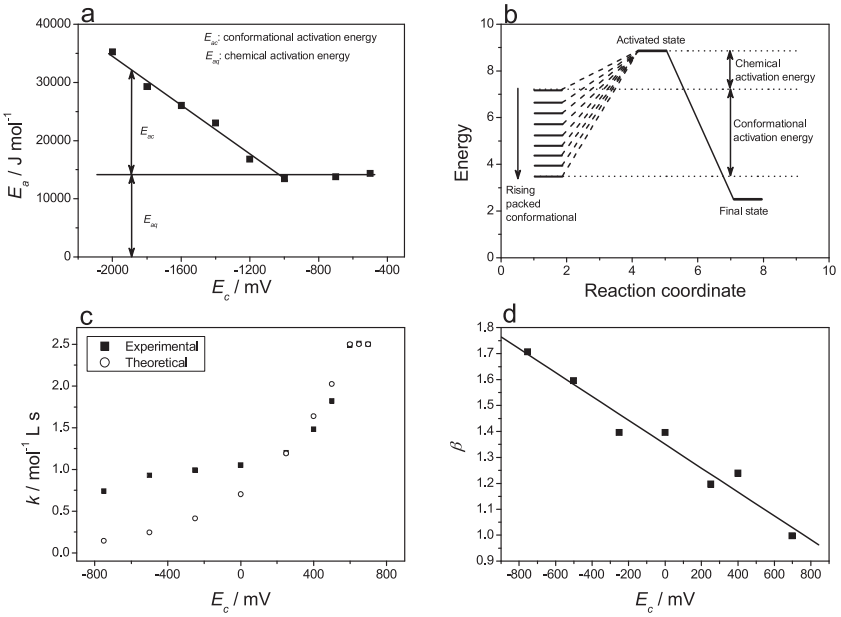

Figure 9. a) Evolution of the experimental activation energy for the polymer oxidation as a function of the cathodic potential of prepolarization for a constant time: rising packed conformations of the initial state at more negative potentials. b) The activation energy for the oxidation is constituted by two components: the constant electrochemical activation energy and the energy required to relax the initial packed conformations of the polymer chains. Panel (a) reproduced with permission.[29] Copyright 2009, Elsevier. Panel (b) reproduced with permission.[31] Copyright 2010, Society of Chemical Industry. c) Evolution of k for different packed conformations attained by polarization at rising negative potentials. d) Linear evolution of β ($\beta = 1.35–4.62 \times 10^{-4} Ec$, the correlation coefficient: $r^2 = 0.98$) at increasing packed initial states. Panels (c,d) reproduced with permission.[26] Copyright 2008, Elsevier.

energy. Then the reaction continues, consuming the chemical activation energy.

Figure 9c shows the evolution of the reaction coefficient as a function of the initial state for the oxidation of polypyrrole films. Open initial states (Figure 1) give a constant value of the reaction coefficient. Initial states of rising packed conformations give decreasing values of the reaction coefficients.

Figure 9d shows the linear variation of the reaction order related to the concentration of active centers in the film as a function of the reduction compaction initial state attained by reduction at rising cathodic overpotentials. Similar results for different conducting polymers were attributed to the interaction of the counterion from the solution during relaxation with an increasing number of active centers when the initial state presents a more packed conformational structure.

The reaction order related to the concentration of counterions in solution (α) is independent of the initial or final structural states for the reaction: it does not include any information about conformational or structural states of the reactive polymer chains.

5. Theoretical Description

Electrochemical models state that the kinetic coefficient of any oxidation reaction is an exponential function of the anodic overpotential η ($\eta = E–E_0$, where E is applied anodic potential and E_0 is the standard oxidation potential of the polymer).[65,66] Any oxidation kinetics are described (for $\eta < 150$ mV) by the Buttler-Volmer equation. After combination with Equation (2) a general electrochemical kinetic equation is attained for reactions involving more than one reactant during the electron transfer:[66]

$$i = k \prod c_j^{\beta,j} \exp\left(\frac{\alpha F \eta}{RT}\right) = k' \prod c_j^{\beta,j} \exp\frac{-E_a}{RT} \quad (15)$$

where c and β, j are the concentration and the reaction order, respectively, associated to the reactant j. The activation energy, E_a, of the reaction is a function of the anodic overpotential, η.

Then, using films of conducting polymers as electroactive materials, both the reaction coefficient, k, and the activation energy, E_a, results in a function of variable (Figure 9) not included in previous chemical or electrochemical kinetic models for oxidation reactions: the cathodic overpotential, η_c ($\eta_c = E–E_c$; E is the applied cathodic potential for the reduction-compaction and E_c is the closing potential of the polymer structure in the studied media) applied to obtain the initial reduced and compacted conformational state for the subsequent oxidation.

Therefore any quantitative description of the electrochemical oxidation kinetics must include a new energetic component controlled by η_c that quantify the structural energy of the initial state. The electrochemically stimulated conformational relaxation (ESCR) model, developed for reactions in conducting polymers,[13,22,44,61,62,98–102,104–109] defines the activation energy as a function of three components:

$$E_a = \Delta H^* + z_c \eta_c - z_r \eta \quad (16)$$

where $z_c\eta_c$ is the conformational activation energy stored by electrochemical reduction and conformational compaction of the polymer chains, which is a linear function of the cathodic overpotential, η_c; z_c is the charge required to reduce and compact one mol of polymeric segments. During oxidation at the anodic overpotential η provides the required energy, $z_r\eta$, to relax the packed conformational structure, allowing the subsequent oxidition and swelling the film, where z_r is the charge required to relax, oxidize, and swell one mol of polymeric segments. The two chemostructural components, $z_c\eta_c$ and $z_r\eta$, are energetic (CV) terms. The magnitudes of z_c and z_r can be empirically obtained for every system polymer/electrolyte.[62,109,110] The term ΔH^* accounts for the energy of the polymer system in absence of any reaction.

Equation (16) describes and fits the experimental results from Figure 9a. The chemical activation energy for the oxidation at a constant anodic overpotential η is independent of the initial state if $\eta_c = 0$, which means that the initial state for the oxidation has an open structure. The activation energy of

the polymer oxidation, when $\eta_c \neq 0$, includes the new term, $z_c\eta_c$, and becomes a linear function of η_c.

By substituting Equation (16) in Equation (15):

$$i = k' \prod c_j^{\beta,j} \exp\left(\frac{-RT - \Delta H^* - z_c\eta_c + z_r\eta}{RT}\right) \quad (17)$$

Equation (17) is a structural electrochemical equation, describing and quantifying reaction rates that induce conformational and structural changes. Moreover, it includes non-structural electrochemical kinetics. For electrochemical oxidations not including structural aspects ($\eta_c = 0$) Equation (17) become the Tafel ($\eta < 10$ mV) or Buttler-Volmer ($\eta < 150$ mV) equation. For higher overpotentials ($\eta > 150$ mV) it includes the energy required to relax, oxidize, and swell the film and provides the required tool to obtain high concentrations of active centers (included by $c_j^{\beta,j}$) in the film. Equation (17) quantifies and describes structural changes (conformational or macroscopic).

From Equation (17), the reaction coefficient:

$$\ln k = \ln k' + \left(\frac{z_r\eta - \Delta H^*}{RT}\right) - \left(\frac{z_c\eta_c}{RT}\right) = k_0\left(\frac{z_r\eta - \Delta H^*}{RT}\right) - \left(\frac{z_c\eta_c}{RT}\right) \quad (18)$$

When the oxidation starts from an initial state with an open structure ($\eta_c = 0$) k becomes independent of η_c, describing experimental results from Figure 9c for initial states attained by reduction at more positive potentials than 600 mV. Rising packed conformations of the initial states, attained by reduction at rising cathodic overpotentials (η_c), will promote an exponential decrease of the reaction coefficient, in good agreement with the experimental results, Figure 9c. Equation (18) is the structural kinetic coefficient, describing and quantifying the influence of conformational and macroscopic structural changes induced by reactions on the kinetic coefficient.

In Equation 17 $\Pi c_i^{\beta,j}$ is the product of the reactant concentrations, $[A^-]\alpha\,[Pol^*]\beta$. By taking logarithms and rearranging:

$$\beta = k'' + \left(z_c\eta_c / RT\,[Pol^*]\right) \quad (19)$$

describing the linear dependence of β from the cathodic overpotential η_c, Figure 9d, and from $(1/[Pol^*])$.

6. Different Materials and Ionic Exchanges

Conducting polymers synthesized in presence of large counterions experience a prevalent exchange of cation during p-dedoping and p-doping:[15,17,22]

$$\left[\left(Pol^0\right)\left(MA^-\right)_n\left(C^+\right)_n\right]_s \rightleftarrows \left[\left(Pol^{n+}\right)\left(MA^-\right)_n\right]_s + n\left(C^+\right)_{aq} + n\left(e^-\right)_{metal} \quad (20)$$

where MA^- represents any macroscopic anion (organic, polymeric, or inorganic) trapped inside the CP during polymerization and C^+ represents a cation (also named coion) required to balance the charge of the trapped macro-anion. Those polymers swell during reduction by entrance of cations and shrink during oxidation by expulsion of cations. The conformational compation of the polymeric chains takes place by oxidation at anodic overpotentials and the conformational relaxation occurs by reduction at cathodic overpotentials. Cathodic chronoamperograms present nucleation-relaxation processes allowing one to obtain the chemical kinetic magnitudes.[106,111]

Reduction reactions related to n-doping processes

$$\underset{\text{Neutral chains}}{\left(Pol^0\right)_s} + n\left(C^+\right)_{aq} + n\left(e^-\right)_{metal} \rightleftarrows \underset{\text{Reduced chains}}{\left[\left(Pol^{n-}\right)_s\left(C^+\right)_n(Solv)_m\right]_{gel}} \quad (21)$$

also follow kinetic Equation (2), being the kinetic influenced by the initial packed state of the "neutral" polymer.[21]

The structural chemical kinetic methodology can be applied to any structural change giving nucleation-like responses on the chronoamperometric responses, as those observed from some carbon nanotubes.[112,113]

6.1. Enzymatic Kinetics, Protein Kinetics, or Ionic Flow Through Ion Channels in Membranes: Conformational Kinetic Control

Figure 4b reproduces the shape of the allosteric kinetics in enzymes or proteins (**Figure 10**A). The free hemo groups reacts with oxygen in a similar way to that of the initial open conformational states during oxidation. The four hemo groups in

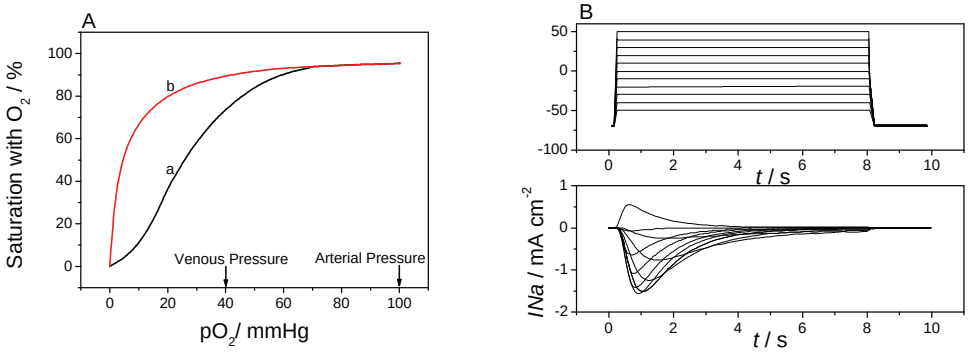

Figure 10. A) The four hemo groups in hemoglobin react with oxygen through four consecutive steps of increasing reaction rates (a). The free hemo groups reacts with oxygen in a similar way to that of the initial open conformational states during oxidation (b). B) Single sodium channel records and family of average Na currents (Iavg) for a series of depolarizations ranging from –50 to +60 mV, starting and ending at –70 mV. Reproduced with permission.[116]

hemoglobin react with oxygen through four consecutive steps of increasing reaction rates explained by the rising open conformational structures allowing faster oxygen access.[114] Allosteric effect arises when the reaction of ligands with one site of any polyvalent molecule affects the reaction of ligand(s) at one or more other sites as a result of conformational changes.[115]

Figure 10B reproduces, at a different scale, pulses of ionic flow across ion channels constituted by biopolymers in membranes.[116] When the Nernst potential gradient across the membrane overcomes the threshold potential, the biopolymer changes its conformational structure (electromechanical property), opening the pore and allowing the ionic flow: the potential drops and the biopolymer recovers the closed structure dropping the ionic flow.

As a conclusion the conformational structure of CPs, enzymes, or proteins control the subsequent reaction rate of its active centers. Similar ionic flow rates, under similar kinetic control of the conformational movements in chains, are produced for charge balance during oxidation in membranes of conducting polymer and during charge balance across ionic channel in biological membranes. It should be expected that a similar theoretical physicochemical description of both processes and a similar quantification of the kinetic magnitudes is involved.

6.2. Structural Chemical Kinetics as a Diagnostic Tool to Characterize Intermolecular Interaction Variations During Reactions

The conformational energy in dense and reactive gels of conducting polymers is mainly defined by the polymer-polymer attractive van der Waals forces in the initial reduced state. Those intermolecular forces move progressively from attractive to repulsive forces along the oxidation, while positive charges are generated along neighbor chains. Repulsive forces and restructuration of the double bonds along the chains promote conformational movements with generation of free volume and entrance of charge-balancing counterions and solvent molecules from the solution for osmotic pressure balance, leading to a final balance of intermolecular forces (polymer-polymer, polymer-ions, polymer-solvent and solvent ions) inside the oxidized film.

The structural chemical kinetics procedure provides a tool to explore those intermolecular forces and its change during reaction. Quantitative relationships between the attained reaction kinetic coefficients in different solvents and those molecular or macroscopic constants of the solvent acting on the intermolecular forces could be expected. If the chemical kinetics are studied in different solvents under identical chemical and electrical conditions, any variation on the attained kinetic coefficient could only be attributed to variations on polymer-solvent and ions-solvent interactions.

7. Conclusions

Electrochemical reactions in films of conducting polymers involve reactive chains exchanging ions and solvent with the electrolyte under current flow. The reaction induces structural changes, i.e., conformational movements in chains and swelling, shrinking, compaction, and relaxation processes in the reactive dense gel.

Oxidation or reduction reaction kinetics can be followed by potential steps. Kinetics obtained from initial states, which have packed conformational structures, present an induction time that is absent when open conformational structures are used as initial states for the reaction.

The initial reaction rates are the slope of the kinetics at time zero when the initial state is an open structure, or the slope at the induction time when the initial state for the reaction presents a packed conformational structure.

By changing one of the chemical variables every time, keeping a constant value for each of the rest, chemical kinetic control of the processes was corroborated, (Equations (8), (10), and (13)) allowing determination of the activation energy, the reaction coefficient, and the reaction orders related to each of the reactants.

The activation energy of the reaction, the reaction coefficient, and the reaction order related to the concentration of active centers in the polymer film (on thepolymer chains) change with the packed conformational structure of the initial state for the reaction. Those magnitudes (E_a, k, and β) include structural information about the initial state of the reaction: the chemical kinetics become structural chemical kinetics.

The experimental results are described by the electrochemically stimulated conformational relaxation (ESCR) model. The activation energy of the reaction includes three components: the oxidation-relaxation energy, $z_r\eta$; the conformational activation energy stored by conformational compaction, $z_c\eta_c$; and the energy of the polymer system in the absence of any reaction, ΔH^*.

The experimental results for the variation of the activation energy, the reaction coefficient, or the reaction order as a function of the conformational compaction of the initial state for the oxidation (defined by the reduction-compation overpotential) fit the theoretical description from the model.

Kinetic responses showing structural effects as a maximum (i/t), or as an induction time ($[Pol^*]/t$), are quite usual from conducting polymers (p-doping or n-doping, exchanging anions, or cations), carbon nanotubes, enzymes, proteins, ionic channels in cells, and most biological processes. The structural chemical kinetics can become a useful tool to develop a predictive model for biological reactions involving conformational movements, water, and ion exchanges with the surrounding, as conducting polymers do.

Acknowledgements

Authors acknowledge financial support from the Spanish Government (MCINN) Project MAT2008-06702, Seneca Foundation Project 08684/PI/08. J.G.M. acknowledges the Spanish Education Ministry for a FPU grant (AP2010-3460).

Received: March 14, 2012
Published online: September 10, 2012

[1] J. A. Irvin, D. J. Irvin, J. D. Stenger-Smith, in *Handbook of Conducting Polymers*, Vol. *2*, (Eds: T. A. Skotheim, R. L. Elsenbaumer, J. R. Reynolds), CRC Press, Boca Raton **2007**.
[2] P. Novak, K. Muller, K. S. V. Santhanam, O. Haas, *Chem. Rev.* **1997**, *97*, 207.

[3] A. L. Dyer, J. R. Reynolds, in *Handbook of Conducting Polymers*, Vol. *2*, (Eds: T. A. Skotheim, R. L. Elsenbaumer, J. R. Reynolds), CRC Press, Boca Raton **2007**.
[4] R. J. Mortimer, A. L. Dyer, J. R. Reynolds, *Displays* **2006**, *27*, 2.
[5] P. Burgmayer, R. W. Murray, *J. Am. Chem. Soc.* **1982**, *104*, 6139.
[6] C. R. Martin, *Science* **1994**, *266*, 1961.
[7] T. F. Otero, E. Angulo, J. Rodriguez, C. Santamaria, *J. Electroanal. Chem.* **1992**, *341*, 369.
[8] E. Smela, *Adv. Mater.* **2003**, *15*, 481.
[9] G. M. Friehs, V. A. Zerris, C. L. Ojakangas, M. R. Fellows, J. P. Donoghue, *Stroke* **2004**, *35*, 2702.
[10] H. B. Mark, N. Atta, Y. L. Ma, K. L. Petticrew, H. Zimmer, Y. Shi, S. K. Lunsford, J. F. Rubinson, A. Galal, *Bioelectrochem. Bioenerg.* **1995**, *38*, 229.
[11] J. Kost, R. Langer, *Adv. Drug Delivery Rev.* **2001**, *46*, 125.
[12] R. D. Keynes, D. J. Aidley, C. L. H. Huang, *Nerve and Muscle*, Cambridge University Press, Cambridge **2011**.
[13] T. F. Otero, in *Modern Aspects of Electrochemistry*, Vol. *33*, (Eds: J. O. Bockris, R. E. White, B. E. Conway), Plenum Press, New York **1999**.
[14] T. F. Otero, in *Structural Biological Materials. Design and Structure-Properties Relationships*, (Eds: M. Elices, R. W. Cahn), Pergamon, Amsterdam **2000**.
[15] T. F. Otero, in *Handbook of Conducting Polymers*, (Eds: T. A. Skotheim, J. R. Reynolds), CRC Press, Boca Raton **2006**.
[16] T. F. Otero, in *Intelligent Materials*, (Eds: M. Shahinpoor, H. J. Schneider), RSC, Oxford **2008**.
[17] T. F. Otero, J. Arias-Pardilla, in *Electropolymerization: Concepts, Materials and Applications*, (Eds: S. Cosnier, A. Karyakin), Wiley-VCH, Weinheim **2010**.
[18] T. F. Otero, in *From Non-Covalent Assemblies to Molecular Machines*, (Eds: J. P. Sauvage, P. Gaspard), Wiley-VCH, Weinheim **2011**.
[19] T. F.Otero, J. G. Martinez, J. Arias-Pardilla, *Electrochim. Acta*, DOI:10.1016/j.electacta.2012.03.097.
[20] J. Arias-Pardilla, T. F. Otero, R. Blanco, J. L. Segura, *Electrochim. Acta* **2010**, *55*, 1535.
[21] J. Arias-Pardilla, W. Walker, F. Wudl, T. F. Otero, *J. Phys. Chem. B* **2010**, *114*, 12777.
[22] L. V. Conzuelo, J. Arias-Pardilla, J. V. Cauich-Rodriguez, M. A. Smit, T. F. Otero, *Sensors* **2010**, *10*, 2638.
[23] T. F. Otero, E. Angulo, *Solid State Ionics* **1993**, *63-5*, 803.
[24] T. F. Otero, S. Villanueva, M. Bengoechea, E. Brillas, J. Carrasco, *Synth. Met.* **1997**, *84*, 183.
[25] T. F. Otero, R. Abadias, *J. Electroanal. Chem.* **2007**, *610*, 96.
[26] T. F. Otero, F. Santos, *Electrochim. Acta* **2008**, *53*, 3166.
[27] T. F. Otero, R. Abadias, *J. Electroanal. Chem.* **2008**, *618*, 39.
[28] T. F. Otero, *J. Mater. Chem.* **2009**, *19*, 681.
[29] T. F. Otero, J. M. G. de Otazo, *Synth. Met.* **2009**, *159*, 681.
[30] T. F. Otero, J. Arias-Pardilla, E. Chermak, *Synth. Met.* **2010**, *160*, 425.
[31] T. F. Otero, M. C. Romero, *Polym. Int.* **2010**, *59*, 329.
[32] H. J. Ahonen, J. Lukkari, J. Kankare, *Macromolecules* **2000**, *33*, 6787.
[33] G. E. Gunbas, P. Camurlu, I. M. Akhmedov, C. Tanyeli, A. M. Onal, L. Toppare, *J. Electroanal. Chem.* **2008**, *615*, 75.
[34] A. R. Hillman, S. J. Daisley, S. Bruckenstein, *Electrochim. Acta* **2008**, *53*, 3763.
[35] N. Levy, M. D. Levi, D. Aurbach, R. Demadrille, A. Pron, *J. Phys. Chem. C* **2010**, *114*, 16823.
[36] S. Link, T. Richter, O. Yurchenko, J. Heinze, S. Ludwigs, *J. Phys. Chem. B* **2010**, *114*, 10703.
[37] Q. B. Pei, G. Zuccarello, M. Ahlskog, O. Inganas, *Polymer* **1994**, *35*, 1347.
[38] M. Sendur, A. Balan, D. Baran, B. Karabay, L. Toppare, *Org. Electron.* **2010**, *11*, 1877.
[39] S. Tarkuc, Y. A. Udum, L. Toppare, *Polymer* **2009**, *50*, 3458.
[40] M. Wagner, C. Kvarnstrom, A. Ivaska, *Electrochim. Acta* **2010**, *55*, 2527.
[41] I. Yamaguchi, H. Mitsuno, *Macromolecules* **2010**, *43*, 9348.
[42] T. Yamamoto, M. Usui, H. Ootsuka, T. Iijima, H. Fukumoto, Y. Sakai, S. Aramaki, H. M. Yamamoto, T. Yagi, H. Tajima, T. Okada, T. Fukuda, A. Emoto, H. Ushijima, M. Hasegawa, H. Ohtsu, *Macromol. Chem. Phys.* **2010**, *211*, 2138.
[43] T. F. Otero, In *Handbook of Organic Conductive Molecules and Polymers* (Ed. H.S. Nalwa), John Wiley&Sons: Chichester, **1997**, pp 517–594.
[44] T. F. Otero, H. Grande, J. Rodriguez, *J. Phys. Chem. B* **1997**, *101*, 8525.
[45] A. Malinauskas, *Ber. Bunsen. Phys. Chem.* **1998**, *102*, 972.
[46] G. Alici, B. Mui, C. Cook, *Sens. Actuators A-Phys.* **2006**, *126*, 396.
[47] G. Alici, N. N. Huynh, *Sens. Actuators A-Phys.* **2006**, *132*, 616.
[48] L. Bay, K. West, P. Sommer-Larsen, S. Skaarup, M. Benslimane, *Adv. Mater.* **2003**, *15*, 310.
[49] M. S. Cho, J. J. Choi, T. S. Kim, Y. Lee, *Sens. Actuators B* **2011**, *156*, 218.
[50] M. Christophersen, B. Shapiro, E. Smela, *Sens. Actuators B* **2006**, *115*, 596.
[51] K. Kaneto, H. Fujisue, M. Kunifusa, W. Takashima, *Smart Mater. Struct.* **2007**, *16*, S250.
[52] R. Kiefer, S. Y. Chu, P. A. Kilmartin, G. A. Bowmaker, R. P. Cooney, J. Travas-Sejdic, *Electrochim. Acta* **2007**, *52*, 2386.
[53] A. Mazzoldi, C. Degl'Innocenti, M. Michelucci, D. De Rossi, *Mater. Sci. Eng. C-Biomimetic Mater., Sens. Syst.* **1998**, *6*, 65.
[54] T. F. Otero, G. V. Arenas, J. J. L. Cascales, *Macromolecules* **2006**, *39*, 9551.
[55] T. F. Otero, J. J. L. Cascales, G. V. Arenas, *Mater. Sci. Eng. C-Biomimetic Supramol. Syst.* **2007**, *27*, 18.
[56] Q. B. Pei, O. Inganas, *J. Phys. Chem.* **1992**, *96*, 10507.
[57] B. H. Qi, W. Lu, B. R. Mattes, *J. Phys. Chem. B* **2004**, *108*, 6222.
[58] J. M. Sansinena, J. B. Gao, H. L. Wang, *Adv. Funct. Mater.* **2003**, *13*, 703.
[59] E. Smela, N. Gadegaard, *Adv. Mater.* **1999**, *11*, 953-+.
[60] G. M. Spinks, L. Liu, G. G. Wallace, D. Z. Zhou, *Adv. Funct. Mater.* **2002**, *12*, 437.
[61] H. Grande, T. F. Otero, *Electrochim. Acta* **1999**, *44*, 1893.
[62] T. F. Otero, H. Grande, *J. Electroanal. Chem.* **1996**, *414*, 171.
[63] C. Odin, M. Nechtschein, *Phys. Rev. Lett.* **1991**, *67*, 1114.
[64] C. Odin, M. Nechtschein, *Synth. Met.* **1993**, *55*, 1287.
[65] A. J. Bard, L. R. Faulkner, *Electrochemical Methods: Fundamentals and Applications*, John Wiley & Sons, Inc., New York **2001**.
[66] K. J. Vetter, *Electrochemical Kinetics. Theoretical Aspects*, Academic Press Inc., New York **1967**.
[67] R. Mazeikiene, A. Malinauskas, *Synth. Met.* **2002**, *129*, 61.
[68] M. Laridjani, J. P. Pouget, E. M. Scherr, A. G. Macdiarmid, M. E. Jozefowicz, A. J. Epstein, *Macromolecules* **1992**, *25*, 4106.
[69] J. Bisquert, *Electrochim. Acta* **2002**, *47*, 2435.
[70] G. Y. Han, G. Q. Shi, *Sens. Actuators B* **2004**, *99*, 525.
[71] K. Aoki, J. A. Cao, Y. Hoshino, *Electrochim. Acta* **1993**, *38*, 1711.
[72] V. Noel, H. Randriamahazaka, C. Chevrot, *J. Electroanal. Chem.* **2003**, *542*, 33.
[73] E. Krivan, C. Visy, J. Kankare, *J. Phys. Chem. B* **2003**, *107*, 1302.
[74] J. Roncali, L. H. Shi, F. Garnier, *J. Phys. Chem.* **1991**, *95*, 8983.
[75] Q. B. Pei, O. Inganas, *J. Phys. Chem.* **1993**, *97*, 6034.
[76] E. Smela, M. Kallenbach, J. Holdenried, *J. Microelectromech. Syst.* **1999**, *8*, 373.
[77] S. Skaarup, K. West, B. Zachauchristiansen, M. A. Careem, G. K. R. Senadeera, *Solid State Ionics* **1994**, *72*, 108.
[78] K. Aoki, M. Kawase, *J. Electroanal. Chem.* **1994**, *377*, 125.
[79] C. Barbero, R. Kotz, M. Kalaji, L. Nyholm, L. M. Peter, *Synth. Met.* **1993**, *55*, 1545.
[80] C. Odin, M. Nechtschein, P. Hapiot, *Synth. Met.* **1992**, *47*, 329.

[81] K. Aoki, J. Cao, Y. Hoshino, *Electrochim. Acta* **1994**, *39*, 2291.
[82] H. Randriamahazaka, T. Bonnotte, V. Noel, P. Martin, J. Ghilane, K. Asaka, J. C. Lacroix, *J. Phys. Chem. B* **2011**, *115*, 205.
[83] M. Lapkowski, M. Zagorska, I. Kulszewiczbajer, A. Pron, *Synth. Met.* **1993**, *55*, 1570.
[84] B. Villeret, M. Nechtschein, *Phys. Rev. Lett.* **1989**, *63*, 1285.
[85] M. A. Vorotyntsev, M. Skompska, E. Pousson, J. Goux, C. Moise, *J. Electroanal. Chem.* **2003**, *552*, 307.
[86] H. Q. Tang, A. Kitani, M. Shiotani, *J. Electroanal. Chem.* **1995**, *396*, 377.
[87] M. Kalaji, L. M. Peter, L. M. Abrantes, J. C. Mesquita, *J. Electroanal. Chem.* **1989**, *274*, 289.
[88] A. R. Hillman, M. A. Mohamoud, S. Bruckenstein, *Electroanalysis* **2005**, *17*, 1421.
[89] P. Borys, M. Lapkowski, J. Zak, Z. J. Grzywna, *Chem. Phys. Lett.* **2007**, *446*, 391.
[90] L. Smilowitz, N. S. Sariciftci, R. Wu, C. Gettinger, A. J. Heeger, F. Wudl, *Phys. Rev. B* **1993**, *47*, 13835.
[91] D. J. Walton, C. E. Hall, A. Chyla, I. V. F. Viney, J. M. Mure, *Synth. Met.* **1993**, *55*, 1465.
[92] D. Posadas, M. Fonticelli, M. J. R. Presa, M. I. Florit, *J. Phys. Chem. B* **2001**, *105*, 2291.
[93] H. Randriamahazaka, C. Plesse, D. Teyssie, C. Chevrot, *Electrochim. Acta* **2005**, *50*, 1515.
[94] K. Aoki, *J. Electroanal. Chem.* **1994**, *373*, 67.
[95] M. Lapkowski, M. D. Levi, *Synth. Met.* **1992**, *51*, 75.
[96] K. Fraoua, M. Delamar, C. P. Andrieux, *J. Electroanal. Chem.* **1996**, *418*, 109.
[97] M. J. R. Presa, D. Posadas, M. I. Florit, *J. Electroanal. Chem.* **2000**, *482*, 117.
[98] T. F. Otero, J. Rodriguez, H. Grande, *J. Braz. Chem. Soc.* **1994**, *5*, 179.
[99] T. F. Otero, H. J. Grande, J. Rodriguez, *J. Phys. Chem. B* **1997**, *101*, 3688.
[100] T. F. Otero, I. Boyano, *J. Phys. Chem. B* **2003**, *107*, 4269.
[101] H. Grande, T. F. Otero, *J. Phys. Chem. B* **1998**, *102*, 7535.
[102] T. F. Otero, H. Grande, J. Rodriguez, *Synth. Met.* **1996**, *76*, 285.
[103] T. F. Otero, J. G. Martinez, K. Hosaka, H. Okuzaki, *J. Electroanal. Chem.* **2011**, *657*, 23.
[104] T. F. Otero, H. Grande, J. Rodriguez, *Electrochim. Acta* **1996**, *41*, 1863.
[105] T. F. Otero, I. Boyano, *J. Phys. Chem. B* **2003**, *107*, 6730.
[106] B. J. West, T. F. Otero, B. Shapiro, E. Smela, *J. Phys. Chem. B* **2009**, *113*, 1277.
[107] T. F. Otero, I. Boyano, *Electrochim. Acta* **2006**, *51*, 6238.
[108] T. F. Otero, J. G. Martinez, *J. Solid St. Electrochem.* **2011**, *15*, 1169.
[109] T. F. Otero, H. Grande, J. Rodriguez, *J. Electroanal. Chem.* **1995**, *394*, 211.
[110] T. F. Otero, H. Grande, J. Rodriguez, *Synth. Met.* **1997**, *85*, 1077.
[111] T. F. Otero, J. Padilla, *J. Electroanal. Chem.* **2004**, *561*, 167.
[112] P. Gimenez, K. Mukai, K. Asaka, K. Hata, H. Oike, T. F. Otero, *Electrochim. Acta* **2012**, *60*, 177.
[113] K. Mukai, K. Asaka, K. Hata, T. F. Otero, H. Oike, *Chem.-Eur J.* **2011**, *17*, 10965.
[114] A. Fersht, *Enzyme Structure and Mechanism*, W. H. Freeman and Company, San Francisco **1977**.
[115] T. Atwood, P. Campbell, H. Parish, T. Smith, J. Stirling, F. Vella, R. Cammack, *Oxford Dictionary of Biochemistry and Molecular Biology*, Oxford University Press, Oxford **2006**.
[116] F. Bezanilla, *The Nerve Impulse*, **1998**, http://nerve.bsd.uchicago.edu/med98a.htm (accessed January **2012)**.